

Differentiating Malignant Glioma from Metastasis Using Regions of Interest Generated by a Novel Diffusion Tensor Segmentation Algorithm

T. L. Jones¹, A. W. Chung², A. J. Lawrence², B. A. Bell¹, and T. R. Barrick²

¹Academic Neurosurgery Unit, St George's University of London, London, United Kingdom, ²Centre for Clinical Neurosciences, St George's University of London, London, United Kingdom

Introduction: Intracranial metastases and primary malignant gliomas (glioblastoma multiforme, GBM) account for the majority of brain tumours in adults. These tumours may have similar contrast enhancement and signal intensity patterns on conventional MRI sequences however management and prognosis varies significantly between the two. Previous studies have identified differences using diffusion tensor imaging (DTI) parameters in manually selected regions of interest (ROI) however their diagnostic role is yet to be fully elucidated [1]. Manual selection of these ROIs typically requires drawing around tumour regions on a slice by slice basis on co registered conventional sequences (e.g. FLAIR, T1 & contrast) which is time consuming and subject to a degree of inter- and intra-observer variability. We describe a novel method of segmenting GBM and metastasis DTI scans using a k-medians algorithm and identifying regions of interest by selecting automatically clustered tumour regions. Using these regions of interest we contrast diffusion patterns between GBM and metastasis and compare results of our novel method with manual ROI delineation.

Methods: *Image Acquisition:* Diffusion tensor axial MR scans were acquired for 27 brain tumour patients (16 GBM, 11 metastases) prior to surgery. Mean age 60 (27-74), 21 male, 7 female. The study was approved by ethics committee and all patients gave written informed consent. Subjects were scanned on a 1.5T General Electric Signa MRI. Diffusion-weighted images were acquired using a single shot spin-echo planar sequence (EPI) with 12 diffusion sensitised directions ($b=1000 \text{ s mm}^2$), as described previously [2]. In plane resolution was 2.5mm and through plane 2.8mm, providing near isotropic voxels. DTIs were computed as described previously [2] and isotropic (p) and anisotropic (q) metrics were calculated for each voxel [3]. In addition, conventional axial T2, FLAIR and gadolinium enhanced T1 sequences were acquired.

Automatic DTI Segmentation - Initial Clustering: To ensure against bias in the clustering, each p and q map was rescaled to contain values between 0 and 1. Initial clustering involved the definition of 16 clusters. These were defined to express the range of tissue types present in brains with intracranial lesions (e.g. normal white matter, cortex, CSF spaces, tumour (solid component, necrotic core), tumour boundary, infiltrating edge and associated oedema, plus partial volume regions). The initial 16 clusters were defined in (p, q) space by the lower quartile, median and upper quartile values for p and q computed across the entire skull stripped brain image, I (Fig-1a). Clusters medians of p and q were then computed.

Image Analysis - K-Medians Clustering: Each image voxel, $i \in I$, was iteratively reclassified to one of the 16 clusters using k-medians clustering based on the distance in (p, q) space of the voxel (p_i, q_i) to its nearest cluster median (m_p, m_q) by,

$$\min_{j \in \{1, \dots, 16\}} \sqrt{(p_i - m_{pj})^2 + (q_i - m_{qj})^2}.$$

This was repeated for 100 iterations with a steady state of classification reached before termination. The final clustering of (p, q) space is shown in Fig-1b

Diffusion Colour Maps (DCM): Median p , q and T2 weighted intensities (T2 values obtained from the $b=0 \text{ s mm}^2$ image) were computed for the final clusters. Median values were ranked according to magnitude to provide 3 grey-scale segmentations with values between 0 and 16 (Fig-1c). RGB colours were assigned to the grey-scale images by assigning the T2 cluster rank to the red channel, the p cluster rank to the green channel and the q cluster rank to the blue channel.

Manual Tumour Segmentation: Using MRICRO software [4], the tumour was manually delineated as the contrast enhancing region on an axial slice by slice basis. Cystic regions (defined by the T2-weighted scan) were excluded (2 cases of malignant glioma). Oedema boundaries were defined by the extent of peritumoural hyper-intensity on T2 weighted images (Fig-2).

Semi-Automatic Region of Interest: Clusters corresponding to tumour and oedema regions were identified in the DCMs. Single points within tumour and oedema regions were input on a slice-by-slice basis to a 2D flood fill algorithm and tumour and oedema maps were output based on the automatic segmentation maps.

Data Collection & Analysis: Median values for p and q were calculated for tumour and oedema regions for each subject and technique. Statistical comparison was performed using a repeated measures MANOVA design incorporating two within subject factors of Technique(manual, semi-automatic) and Region(tumour, oedema) and one between subject factor Tumour(Metastasis, GBM). Two dependent variables investigated (p and q). MANOVA assumptions were met.

Results: Application of the semi-automatic technique to our DCM images generates tumour and oedema ROIs which appear comparable to manually delineated regions (Fig-2). In the oedema region, p is increased in metastases relative to GBM whilst in tumour there is significantly higher q in GBM than metastases (Pillai's Trace, $F(2,24)=25.00, p<0.001$). No significant difference was found between techniques (Pillai's Trace, $F=1.43, p = 0.26$).

Discussion: Higher isotropy in metastatic oedema than GBM may contrast the fluid-rich vasogenic oedema of metastases with infiltrative cellular oedema of GBM. Higher anisotropy within GBM tumour regions may represent a higher cellular proliferation within these lesions. The comparable ROIs generated using our technique validate its use in investigating diffusion parameters between tumour regions of interest. With further validation, these findings may be incorporated into a diagnostic model for tumour type. Accurate delineation of tumour regions is critical in planning resection and radiotherapy margins as well as monitoring subtle changes in size over time. Our method has the advantage of identifying characteristic diffusion patterns, is faster than manual techniques and has intrinsically less observer variability as boundaries are defined automatically.

References: [1] Lu S et al., *AJNR Am J Neuroradiol* 24:937-941, 2003.
[3] Pena A et al., *Br J Radiol* 79:101-109, 2006.

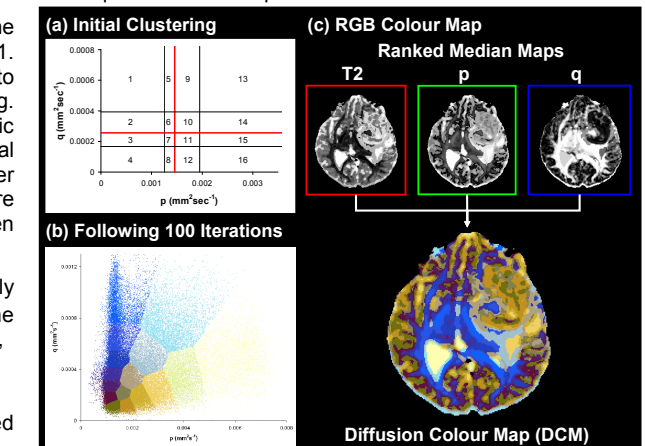


Figure 1: (a) Initial clustering (red lines; medians, black lines; lower & upper quartiles). (b) Clusters after 100 iterations. (c) DCM generation.

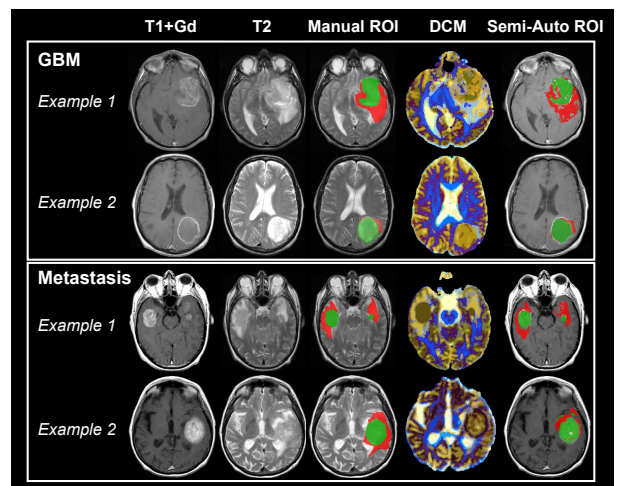


Figure 2: Representative examples of GBM and metastasis (T1+Gd, T2, DCM). Green = tumour and red = oedema.

[2] Clark CA et al., *Neuroimage* 20:1601-1608, 2003.
[4] Rorden C & Brett M, *Behav Neurol* 12:191-200, 2000.